European Journal of Research in Dentistry 2022; 6(2): 73-79
DOI: http://dx.doi.org/10.29228/erd.29

ORIGINAL ARTICLE / ARAŞTIRMA MAKALESİ

Evaluation of the Inferior Alveolar Nerve with 3 Tesla Turbo Spin Echo Magnetic Resonance Imaging

Inferior Alveolar Sinirin 3 Tesla Turbo Spin Eko Manyetik Rezonans Görüntüleme Yöntemiyle Değerlendirilmesi

Melisa OCBE[1], Mehmet Oguz BORAHAN[2], Nuri Cagatay CIMSIT[3]

ABSTRACT

Objectives: The purpose of this study is to evaluate the inferior alveolar nerve's position and nerve plexus within the mandibular canal (MC) with turbo spin echo (TSE) sequences of magnetic resonance imaging (MRI).

Methods: The IAN position was evaluated retrospectively in 220 patients as right and left mandibles (n=440). IAN was classified according to topographical features and branches. MRI images were evaluated as the sequences of T1-weighted, T2-weighted and Proton Density TSE images with standard scanning protocols. Additionally, location of the nerve plexus was recorded as anterior, premolar, molar and retromolar regions.

Results: Patient age was in the range of 7-81 years and the mean age was 37.23 ±16.38. Most common type was Type I (75.2%) which identifies a single major branch of IAN, followed by Type II (21.8%) that identifies inferiorly located and extended branching IAN, and Type III (3%) which represents IAN divides posteriorly into two major branches. Also, it was found that molar region nerve plexus (66.2%) was significantly higher than other regions.

Conclusions: MRI is a non-invasive soft tissue imaging method and is an alternative promising modality regarding in the evaluation of IAN. Preoperative MRI examination may help surgical planning of mandible molar region to avoid complications.

Keywords: inferior alveolar nerve, mandible, mandibular canal, magnetic resonance imaging, turbo spin echo

ÖZ

Giriş: Bu çalışmanın amacı inferior alveolar sinirin konumunu ve mandibular kanalın içerisindeki sinir demetinin morfolojik sınıflamasını turbo spin eko manyetik rezonans görüntüleme (TSE MRG) ile değerlendirmektir.

Materyal ve Metod: Inferior alveolar sinirin konumu, 220 hastaya ait manyetik rezonans görüntülerinde sağ ve sol olarak (n=440) retrospektif olarak sagittal, koronal ve aksiyal kesitlerde değerlendirilmiştir. Inferior alveolar sinir topografik özelliklerine ve dallanmalarına göre sınıflandırılmıştır. Manyetik rezonans görüntüleri T1 ağırlıklı, T2 ağırlıklı, Proton Density olarak kaydedilmiştir. Sinir pleksusunun konumu anterior, premolar, molar, retromolar olarak kaydedilmiştir.

Bulgular: Yaş aralığı 7-81 ve yaş ortalaması 37.23±16.38 olmuştur. En sık görülen inferior alveolar sinir, tek bir sinir dalını ifade eden Tip I (75.2%) olmuştur. İkinci en sık görülen Tip II (%21.8) olup, mandibulanın inferiorundan geçen, uzamış sinir dallanmaları izlenen tipi olmuştur. Posteriorda iki ana dala ayrılan inferior alveolar sinir tipi Tip III olup, görülme sıklığı %3 olarak saptanmıştır. En sık görülen sinir demeti bölgesi molar bölge (%66.2) olarak bulunmuştur.

Sonuç: MRG, invaziv olmayan bir yumuşak doku görüntüleme yöntemi olup inferior alveolar siniri görüntülemede alternatif bir yardımcı yöntem olabilir. Preopertatif olarak MRG, mandibula molar bölgenin cerrahi planlamasında kullanılabilir.

Anahtar Kelimeler: inferior alveolar sinir, mandibula, mandibular kanal, manyetik rezonans görüntüleme, turbo spin eko

Melisa Ocbe (✉)
Marmara Üniversitesi Recep Tayyip Erdoğan Külliyesi Sağlık Yerleşkesi, Diş Hekimliği Fakültesi, Başıbüyük Yolu 9/3 34854 Başıbüyük / Maltepe / İstanbul
e-mail: melisabozkurtt@windowslive.com

Mehmet Oguz Borahan
Assoc. Prof. Dr., Marmara University, Faculty of Dentistry, Department of Oral and Maxillofacial Radiology, Istanbul, Turkey

Nuri Cagatay Cimsit
Prof. Dr., Marmara University, School of Medicine, Internal Medical Sciences, Department of Radiology, Istanbul, Turkey

Submitted / Gönderilme: 08.09.2022 **Accepted/Kabul:** 23.11.2022

INTRODUCTION

Inferior alveolar nerve (IAN) lies inside the mandibular canal (MC) with vascular tissue and it is the largest branch

of the mandibular division of the trigeminal nerve (Kim et al., 2009). Histological sections had shown that the IAN is observed as the fusion of numerous arteries, veins and nerve fibers collected in the connective tissue and located in the upper and lateral parts of the main mandibular nerve trunk. As the inferior alveolar vein and artery runs above the inferior alveolar nerve, surgical interventions to the superior part of the mandibular canal may also affect these vascular tissues as well (Fukami et al., 2012). This is the reason of the course and location of IAN are great interest of dental clinicians.

The topography of the IAN has been tried to be understood by various methods. Although there is no consensus about the course and topography of IAN, there are two approaches for investigating the character and configuration of the inferior alveolar nerve: cadaver studies and imaging methods. As the technological advances progress, imaging methods have been improved and diversified (Weck et al., 2016).

Currently, there are various imaging methods for evaluation of IAN: panoramic radiography (Juodzbalys and Wang, 2010; Weck et al., 2016), computed tomography (CT) and cone beam computed tomography (CBCT) (Imamura et al., 2004; Juodzbalys and Wang, 2010; Chau, 2012; de Oliveira Santos et al., 2012; Ogawa et al., 2016), ultrasonography (USG) (Machtei et al., 2010), endoscopy (Beltrán et al., 2012) and magnetic resonance imaging (MRI) (Nasel et al., 1998; Imamura et al., 2004; Eggers et al., 2005; Ferreti et al., 2009; Krasny et al., 2012; Assaf et al., 2014; Agbaje et al., 2017; Deepho et al., 2017; Kreutner et al., 2017; Deepho et al., 2018; Wamasing et al., 2019; Beck et al., 2019). Panoramic radiography, CT and CBCT can view the mandibular canal cortex, but these imaging methods are not adequate for the interior neurovascular tissue. Traditional radiographs or CBCT may not represent the actual appearance of the bone structure. IAN might not be visible due to the higher interaction of the radiation with the cortical bone rather than trabecular bone. Also, sparse trabeculation of mandibular bone is an inhibitory feature of CBCT image quality. For all these reasons MRI is a superior method with the imaging of neurovascular tissues compared to CBCT (Cavalcanti et al., 1999; Couture et al., 2003).

The purpose of this study is to verify the topography of the inferior alveolar nerve, artery and vein therein by MR imaging method retrospectively.

MATERIAL AND METHODS

Ethical approval for this retrospective study was granted by the Marmara University, Faculty of Medicine, Ethical Committee of Non-invasive Clinical Research with the following project no: 09202272.

MRI images of 220 patients (48 male and 172 female, mean age was 37.23, age range was 7-81) from the archive of Marmara University Medical Hospital, Department of Radiology were collected from the years between 2014 and 2021 for this retrospective study. Aimed region of the interest was also recorded as following modalities: cervical, temporal, facial and temporomandibular MRI.

In the cases with the absence of informed consent form which refers using images for research and scientific reasons, poor qualified images (metal artefacts, movement artefacts, artefacts caused by head stabilizer of MRI machine), insufficient region of interest, presence of any unilateral/bilateral pathologies (tumours, cysts), malformations of mandible or disorders that changes location or branching pattern of MC (e.g. fibrous dysplasia, floride osseous dysplasia, von Recklinghousen disease), presence of postoperative reconstructive or fixative materials, presence of mandibular or bimaxillary orthodontic wire, presence of impacted or partially erupted teeth were excluded from this study.

Procedures

Imaging of the mandible was performed with 3.0-T (MagnetomVerio, Siemens Healthcare, Erlangen, Germany) as standard procedure in all MRI scans with a standard Siemens multicoil. Routine MRI protocol of turbo spin echo (TSE) sequences [T1-weighted (T1w), T2-weighted (T2w), Proton density (PD)] were used in order to evaluate the location and branches of IAN (Table 1).

Table 1: Scanning protocol parameters.

Scan Parameters	T1 weighted	T2 weighted	Proton Density
Matrix size (mm)	295 x 229	240 x 220	240 x 205
FOV (mm)	178 x 178	150 x 150	150 x 150
FA	90	90	90
TR	450	2500	2000
TE	7	80	21

Image Analysis

DICOM file form of images were transferred for reconstruction as sagittal, coronal and axial. The image analysis was performed by using INFINITT software (Version 3.0.11.4 BN11, INFINITT Heathcare Co., Ltd, South Korea).

To ensure efficient evaluation, a clinician (MO) in the Department of Oral Diagnosis and Radiology evaluated the images. During meetings for the pilot study, a specialist working in the Department of Radiology, Faculty of Medicine trained the radiology specialists, and an agreement on the objective criteria for the qualitative evaluation of the images was forged among the evaluators.

For the evaluation of the IAN, classification of Carter and Keen was used (Carter and Keen, 1971). IAN was evaluated bilaterally and Type I (Figure 1 and 4) was used to identify one major branch of IAN which is located nearby the roots of mandibular molars. Type II (Figure 2) was used to represent the IAN located inferiorly. In this type, nutrient canals were seen prolonged, extended and more obliquely run to the superior of the mandible. Type III (Figure 3) presents the IAN type which divides in two major branches in posterior region.

Also, distribution of nerve plexus was classified according to their area such as molar region, retromolar region, premolar region and anterior region.

Figure 1. Type I, sagittal cross section 3T TSE MRI **a;** T1w **b;** T2w **c;** Proton Density

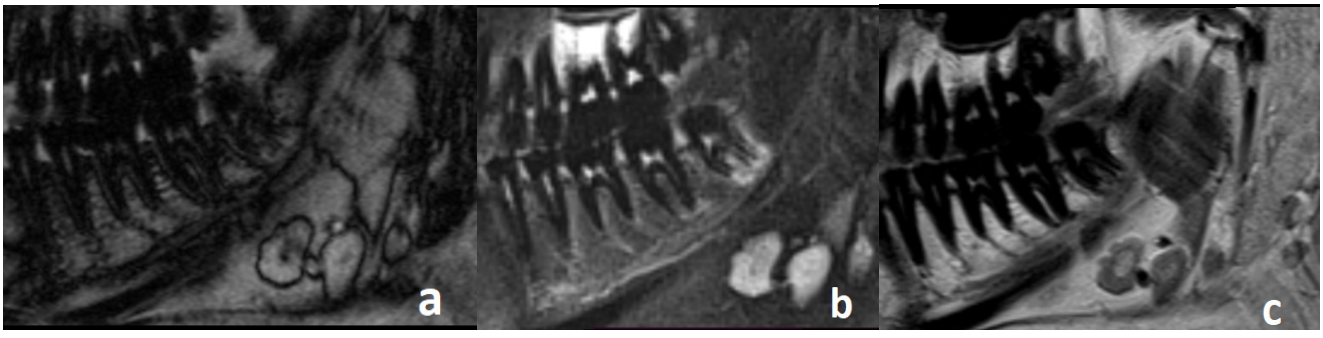

Figure 2. Type II, sagittal cross section 3T TSE MRI **a;** T1w **b;** T2w **c;** Proton Density

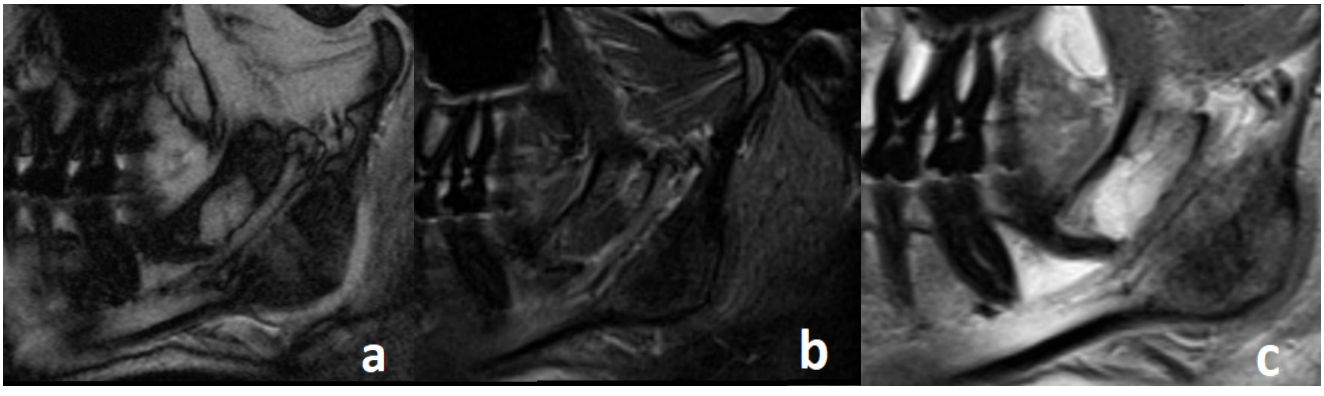

Figure 3. Type III, sagittal cross section 3T TSE MRI **a;** T1w **b;** T2w **c;** Proton Density

RESULTS

There was a statistically significant difference between age groups in terms of IAN Morphology classifications (p:0.002; p<0.05). Type I rate (84.1%) in the 36-45 age group is significantly higher than patients younger than 25 years old (65.2%) and 26-35 years old (71.3%). The rate of Type I over the age of 45 (81.4%) is significantly higher than the group under the age of 25 (65.2%). The rate of Type II under 25 years old (33.3%) is significantly higher than 36-45 years old (13.6%) and over 45 years old (14.3%). There was no significant difference between other age groups (p>0.05).

There was no statistically significant difference between the genders, between right and left sides, between sequences in terms of IAN morphological classifications (p>0.05).

Although it is close to significance between modalities in terms of IAN morphological classifications, there is no statistically significant difference (p>0.05). Hence the difference was not significant, it is noteworthy that the incidence of Type II in the facial MRI (50%) is higher than in the cervical MRI (10.5%) and temporal MRI (0%) (Table 2).

Table 2: Assessments on inferior alveolar nerve parameters.

		Type 1	Type 2	Type 3	
		n (%)	n (%)	n (%)	p
Age groups	< 25	86 (%65,2)	44 (%33,3)	2 (%1,5)	0,002*
	26-35	57 (%71,3)	20 (%25)	3 (%3,8)	
	36-45	74 (%84,1)	12 (%13,6)	2 (%2,3)	
	> 45	114 (%81,4)	20 (%14,3)	6 (%4,3)	
Gender	Female	255 (%74,1)	76 (%22,1)	13 (%3,8)	0,140
	Male	76 (%79,2)	20 (%20,8)	0 (%0)	
Side	Right	167 (%75,9)	46 (%20,9)	7 (%3,2)	0,873
	Left	164 (%74,5)	50 (%22,7)	6 (%2,7)	
Sequence	T1 – weighted	133 (%72,7)	43 (%23,5)	7 (%3,8)	0,527
	T2 – weighted	33 (%70,2)	12 (%25,5)	2 (%4,3)	
	Proton Density	165 (%78,6)	41 (%19,5)	4 (%1,9)	
Modality	Cervical MRI	34 (%89,5)	4 (%10,5)	0 (%0)	0,061
	Temporal MRI	10 (%100)	0 (%0)	0 (%0)	
	Facial MRI	4 (%50)	4 (%50)	0 (%0)	
	Temporomandibular MRI	283 (%73,7)	88 (%22,9)	13 (%3,4)	

Chi-square test **p<0.05*

DISCUSSION

Classification of inferior alveolar nerve anatomy as a cadaveric study was made initially by Olivier. In this study, the anatomy of the inferior alveolar nerve is divided into two categories on 50 cadavers; Type I as the only structural formation with the branches that reach to the teeth (66%) and Type II as the inferior alveolar nerve that forms the plexus that supplies the teeth (34%) (Olivier, 1928). Polland et al. examined 7 cadavers to examine the anatomy of the inferior alveolar nerve. They found a single large nerve bundle in each case (Polland et al., 2001).

Kieser et al. studied one hundred and seven edentulous mandible cadavers to examine the vertical position of the inferior alveolar nerve and its intraosseous branches. They classified IAN as high, if the nerve is located superiorly to the half of the mandibular corpus and as low if it is located in the middle of the mandibular corpus or close to the inferior border of the mandible. Also, IAN were divided into 4 categories according to the branching pattern in the study of Kieser et al. (Kieser et al., 2005). Type I is a single nerve branch, Type II represents a single nerve with small branches, Type III is a form of IAN which gives branches to the molar region in the proximal half of the nerve. Finally, Type IV represents two plexuses in the proximal and distal half of the IAN. According to the study of Kieser et al., the most common type II (56%) is followed by type III (23.3%), type IV (16.9%), and type I (3.8%), respectively. They also reported that 70% of them were localized “low” in the half of the mandible corpus (Kieser et al., 2005). However, Nortjeșet al. found this positioning in 52.2% of the cases. Although, their study of 3,612 radiographs failed to distinguish between dentulous and edentulous subjects, making comparisons with the study of Kieser et al. is difficult (Notrje et al., 1977; Kieser et al., 2005). Additionally, another study of Kieser et al. revealed that a molar plexus from the proximal half of the IAN was the most observed pattern of distribution (Kieser et al., 2004).

Carter and Keen examined the anatomy of the inferior alveolar nerve in their study on 8 cadavers. In this study, they found three types of inferior alveolar nerve trace as Type I, II and III (Table 3). Carter and Keen classification was used in this study (Carter and Keen, 1971).

Table 3: Classification of Carter and Keen (Carter and Keen, 1971)

Type I	Type II	Type III
Single major inferior alveolar nerve that runs within the bony canal.	Inferior alveolar nerve located slightly below the mandible; compared to Type I, dental branches arise more posteriorly, resulting in longer and more oblique.	Inferior alveolar nerve divides posteriorly into two major branches.

It is confirmed that the course and position of IAN can be seen with various sequences of MRI and detectability is higher than CT/CBCT (Imamura et al., 2004; Krasny et al., 2012; Beck et al., 2021; Burian et al., 2020). In this present study sagittal T1w, T2w, PD TSE MRI images were selected. Bone marrow was seen with high signal intensity in T1w sequence images. The cortical bone and its PD were low signal intensity. The MC was low signal intensity inside bone marrow that had high signal intensity. This study reveals that the course of IAN / MC can be detected with MRI TSE sequences. Also, according to the study Murakami et al. detectability of tumour or inflammation with T2w sequence is high but MC and alveolar bone could not be clearly imaged due to the low signal-to-noise ratio (Murakami et al., 1996). In line with this data, we used limited T2w sequence images for this study. Additionally, low detectability of the MC in molar region with CT was shown in the study of Imamura et al. (Imamura et al., 2004). Molar region plexus was the common branching pattern in out study with MRI. This data represents the superior features of MRI. Furthermore, this result is also similar with Kieser et al. classification (Kieser et al., 2004; Kieser et al., 2005).

Both dentulous and edentulous patients were included in this study. In previous studies, as in our study, it was unknown how long the individuals had been edentulous. As represented in the studies of Kieser et al., it is difficult to build consensus regarding the effect of the duration of absence of teeth on the course and distribution of the IAN. Thus, no data could be obtained about the inferior alveolar canal located low or high in this study. Carter and Keen classification was evaluated according to its relation to the teeth in dentulous patients (Carter and Keen, 1971; Nortjé et al., 1977; Kieser et al., 2004; Kieser et al., 2005).

Type I (75.2%) was the most common configuration of IAN in our study, following with Type II (21.8%) and Type III (%3). Small branches of IAN were found 92.3% of total semi-mandibles. These branches were also classified according to their region. The most common plexus type was found as molar plexus (66.2%) followed by retromolar plexus (25.7%), premolar plexus (5.4%) and anterior plexus (2.7%). A study of Chau showed that the IAN was difficult to identify in the first and second lower molar regions with CBCT and Chau found a significant difference between the numbers of CBCT (8.62%) and the number of MRI (0.03%) images that could not reveal the IAN. As the most common plexus was molar plexus with our MRI study, the result of our study also supports Chau's (Chau, 2011).

Some limitations of this study can be considered as, the evaluation of various imaging modalities with different regions of interest. This variety can have an effect on the detection of the neurovascular bundle. However, this distribution of imaging modalities is sufficient for the commonly used MRI images, given that the aim of the study was not to develop a new imaging modality for IAN itself. Also, panoramic reconstruction of MRI images was not used for this study on purpose. Further studies can use multiplanar MRI images (Burian et al., 2020) for the detection of IAN morphology.

CONCLUSIONS

This present study aimed to demonstrate the location of inferior alveolar nerve for preoperative planning of mandible molar region and this study reveals that the course of IAN / MC can be detected with MRI TSE sequences. MRI is an alternative imaging method when the position and course of the nerve cannot be visualized on two-dimensional radiographs or CBCT due to the low cortication of MC. Yet MRI is not very accessible for dentists, patients' previous MRI images that taken for medical reasons can be used by dentists without scanning the patient again. Imaging IAN with MRI is advantageous due to the high image contrast between IAN and bone structures of mandible. Even considering that CBCT involves ionizing radiation, as demonstrated by this study that it is possible to identify the IAN course and position using previous images of the patient, as MRI is a promising imaging method.

Acknowledgements

None.

Conflict of Interest

All authors declare that there are no conflicts of interest.

REFERENCES

1. Agbaje JO, de Casteele EV, Salem AS, Anumendem D, Lambrichts I, Politis C. Tracking of the inferior alveolar nerve: its implication in surgical planning. Clin Oral Investig. 2017

Sep;21(7):2213-2220. doi: 10.1007/s00784.016.2014-x. Epub 2016 Nov 22. PMID: 27878463.

2. Assaf AT, Zrnc TA, Remus CC, Schönfeld M, Habermann CR, Riecke B, Friedrich RE, Fiehler J, Heiland M, Sedlacik J. Evaluation of four different optimized magnetic-resonance-imaging sequences for visualization of dental and maxillo-mandibular structures at 3 T. J Craniomaxillofac Surg. 2014 Oct;42(7):1356-63. doi: 10.1016/j.jcms.2014.03.026. Epub 2014 Apr 13. PMID: 24837485.
3. Beck F, Austermann S, Bertl K, Ulm C, Lettner S, Toelly A, Gahleitner A. Is MRI a viable alternative to CT/CBCT to identify the course of the inferior alveolar nerve in relation to the roots of the third molars? Clin Oral Investig. 2021 Jun;25(6):3861-3871. doi: 10.1007/s00784.020.03716-4. Epub 2020 Dec 7. PMID: 33289048; PMCID: PMC8137481.
4. Beltrán V, Fuentes R, Engelke W. Endoscopic visualization of anatomic structures as a support tool in oral surgery and implantology. J Oral Maxillofac Surg. 2012 Jan;70(1):e1-6. doi: 10.1016/j.joms.2011.09.011. PMID: 22182657.
5. Burian E, Probst FA, Weidlich D, Cornelius CP, Maier L, Robl T, Zimmer C, Karampinos DC, Ritschl LM, Probst M. MRI of the inferior alveolar nerve and lingual nerve-anatomical variation and morphometric benchmark values of nerve diameters in healthy subjects. Clin Oral Investig. 2020 Aug;24(8):2625-2634. doi: 10.1007/s00784.019.03120-7. Epub 2019 Nov 8. PMID: 31705309.
6. Carter RB, Keen EN. The intramandibular course of the inferior alveolar nerve. J Anat. 1971; 108: 433-440.
7. Cavalcanti MG, Ruprecht A, Johnson WT, Southard TE, Jakobsen J. Radiologic interpretation of bone striae: an experimental study in vitro. Oral Surg Oral Med Oral Pathol Oral Radiol Endod. 1999 Sep;88(3):353-7. doi: 10.1016/s1079-2104(99)70042-9. PMID: 10503868.
8. Chau A. Comparison between the use of magnetic resonance imaging and cone beam computed tomography for mandibular nerve identification. Clin Oral Implants Res. 2012 Feb;23(2):253-256. doi: 10.1111/j.1600-0501.2011.02188.x. Epub 2011 Apr 13. PMID: 21488971.
9. Couture RA, Whiting BR, Hildebolt CF, Dixon DA. Visibility of trabecular structures in oral radiographs. Oral Surg Oral Med Oral Pathol Oral Radiol Endod. 2003 Dec;96(6):764-71. doi: 10.1016/j.tripleo.2003.08.013. PMID: 14676770.
10. de Oliveira-Santos C, Souza PH, de Azambuja Berti-Couto S, Stinkens L, Moyaert K, Rubira-Bullen IR, Jacobs R. Assessment of variations of the mandibular canal through cone beam computed tomography. Clin Oral Investig. 2012 Apr;16(2):387-93. doi: 10.1007/s00784.011.0544-9. Epub 2011 Mar 30. PMID: 21448636.
11. Deepho C, Watanabe H, Kotaki S, Sakamoto J, Sumi Y, Kurabayashi T. Utility of fusion volumetric images from computed tomography and magnetic resonance imaging for localizing the mandibular canal. Dentomaxillofac Radiol. 2017 Mar;46(3):20160383. doi: 10.1259/dmfr.20160383. Epub 2017 Feb 17. PMID: 28045346; PMCID: PMC5606273.
12. Deepho C, Watanabe H, Sakamoto J, Kurabayashi T. Mandibular canal visibility using a plain volumetric interpolated breath-hold examination sequence in MRI. Dentomaxillofac Radiol. 2018 Jan;47(1):20170245. doi: 10.1259/dmfr.20170245. Epub 2017 Oct 20. PMID: 28959898; PMCID: PMC5965732.
13. Eggers G, Rieker M, Fiebach J, Kress B, Dickhaus H, Hassfeld S. Geometric accuracy of magnetic resonance imaging of the mandibular nerve. Dentomaxillofac Radiol. 2005 Sep;34(5):285-91. doi: 10.1259/dmfr/89236515. PMID: 16120878.
14. Ferretti F, Malventi M, Malasoma R. Dental magnetic resonance imaging: study of impacted mandibular third molars. Dentomaxillofac Radiol. 2009 Sep;38(6):387-92. doi: 10.1259/dmfr/29929241. PMID: 19700532.
15. Fukami K, Shiozaki K, Mishima A, Kuribayashi A, Hamada Y, Kobayashi K. Bifid mandibular canal: confirmation of limited cone beam CT findings by gross anatomical and histological investigations. Dentomaxillofac Radiol. 2012; 41:460 – 465.
16. Imamura H, Sato H, Matsuura T, Ishikawa M, Zeze R. A comparative study of computed tomography and magnetic resonance imaging for the detection of mandibular canals and cross-sectional areas in diagnosis prior to dental implant treatment. Clin Implant Dent Relat Res. 2004;6(2):75-81. doi: 10.1111/j.1708-8208.2004.tb00029.x. PMID: 15669707.
17. Juodzbalys G, Wang HL. Identification of the mandibular vital structures: practical clinical applications of anatomy and radiological examination methods. J Oral Maxillofac Res. 2010 Jul 1;1(2):e1. doi: 10.5037/jomr.2010.1201. PMID: 24421966; PMCID: PMC3886050.
18. Kieser J, Kieser D, Hauman T. The course and distribution of the inferior alveolar nerve in the edentulous mandible. J Craniofac Surg. 2005;16(1):6-9.
19. Kieser JA, Paulin M, Law B. Intrabony course of the inferior alveolar nerve in the edentulous mandible. Clin Anat. 2004 Mar;17(2):107-11. doi: 10.1002/ca.10196. PMID: 14974097.
20. Kim ST, Hu KS, Song WC, Kang MK, Park HD, Kim HJ. Location of the mandibular canal and the topography of its neurovascular structures. J Craniofac Surg. 2009; 20:936–939.
21. Krasny A, Krasny N, Prescher A. Study of inferior dental canal and its contents using high-resolution magnetic resonance imaging. Surg Radiol Anat. 2012 Oct;34(8):687-93. doi: 10.1007/s00276.011.0910-y. Epub 2011 Dec 6. PMID: 22143348.
22. Kreutner J, Hopfgartner A, Weber D, Boldt J, Rottner K, Richter E, et al. High isotropic resolution magnetic resonance imaging of the mandibular canal at 1.5 T: a comparison of gradient and spin echo sequences. Dentomaxillofac Radiol 2017; 46: 20160268.
23. Machtei EE, Zigdon H, Levin L, Peled M. Novel ultrasonic device to measure the distance from the bottom of the osteotome to various anatomic landmarks. J Periodontol. 2010 Jul;81(7):1051-5. doi: 10.1902/jop.2010.090621. PMID: 20214439.
24. Murakami S, Maeda Y, Fuchihata H. The role of magnetic resonance imaging in preoperative examination for dental implant. J Jpn Soc Oral Implant 1996; 9:24–28.
25. Nasel C, Gahleitner A, Breitenseher M, Czerny C, Glaser C, Solar P, Imhof H. Localization of the mandibular neurovascular bundle using dental magnetic resonance

imaging. Dentomaxillofac Radiol. 1998 Sep;27(5):305-7. doi: 10.1038/sj/dmfr/4600379. PMID: 9879221.

26. Nortjé CJ, Farman AG, Grotepass FW. Variations in the normal anatomy of the inferior dental (mandibular) canal: a retrospective study of panoramic radiographs from 3612 routine dental patients. Br J Oral Surg. 1977 Jul;15(1):55-63. doi: 10.1016/0007-117x(77)90008-7. PMID: 268217.
27. Ogawa A, Fukuta Y, Nakasato H, Nakasato S. Evaluation by dental cone-beam computed tomography of the incidence and sites of branches of the inferior dental canal that supply mandibular third molars. British Journal of Oral and Maxillofacial Surgery, 2016 54(10), 1116–1120. doi:10.1016/j.bjoms.2016.08.007
28. Olivier E. The inferior dental canal and its nerve in the adult. Br Dent J. 1928; 49:356 –358.
29. Polland KE, Munro S, Reford G, Lockhart A, Logan G, Brocklebank L, McDonald SW. The mandibular canal of the edentulous jaw. Clin Anat. 2001;14(6):445-52
30. Wamasing P, Deepho C, Watanabe H, Hayashi Y, Sakamoto J, Kurabayashi T. Imaging the bifid mandibular canal using high resolution MRI. Dentomaxillofac Radiol. 2019 Mar;48(3):20180305. doi: 10.1259/dmfr.20180305. Epub 2018 Nov 7. PMID: 30346803; PMCID: PMC6476361.
31. Weckx A, Agbaje JO, Sun Y, Jacobs R, Politis C. Visualization techniques of the inferior alveolar nerve (IAN): a narrative review. Surg Radiol Anat. 2016 Jan;38(1):55-63. doi: 10.1007/s00276.015.1510-z. Epub 2015 Jul 12. PMID: 26163825; PMCID: PMC4744261.

How to cite this article: Ocbe M, Borahan MO, Cimsit NC. Evaluation of the Inferior Alveolar Nerve with 3 Tesla Turbo Spin Echo Magnetic Resonance Imaging. European Journal of Research in Dentistry, 2022; 6 (2) : 73-79. DOI: http://dx.doi.org/10.29228/erd.29